International Journal of Architectural, Civil and Construction Sciences
ISSN: 2415-1734
Vol:2, No:5, 2008

Experimental Estimation of Mixed-Mode Fracture Properties of Steel Weld

S. R. Hosseini, N. Choupani, and A. R. M. Gharabaghi

***Abstract*—**The modified Arcan fixture was used in order to investigate the mixed mode fracture properties of high strength steel butt weld through experimental and numerical analysis. The fixture consisted of a central section with "butterfly-shaped" specimen that had central crack. The specimens were under pure mode I (opening), pure mode II (shearing) and all in plane mixed mode loading angles starting from 0 to 90 degrees. The geometric calibration factors were calculated with the aid of finite element analysis for various loading mode and different crack length ($0.45\leq a/w \leq 0.55$) and the critical fracture loads obtained experimentally. The critical fracture toughness (K_{IC} & K_{IIC}) estimated with experimental and numerical analysis under mixed mode loading conditions.

***Keywords*—**Arcan specimen, fracture toughness, mixed mode, steel weld.

I. Introduction

THE main objective of this study is to determine a fracture criterion for high tensile steel butt welded joint that used in fixed offshore platform joints and evaluation of strategies for the assessment of structures containing crack-like defects. The mixed-mode fracture mechanics predicts critical state under conditions that crack tip deflection is under opening (mode-I), in-plane shear (mode-II) and out-plane shear (mode-III). It always relates the three basic modes of fracture to loading form as shown in Fig. 1 [1]. Furthermore, it is assumed that the fracture propagates in the pre-existing crack plane. This research is devoted to estimate fracture criterions under pure mode-I, II and in plane mixed mode loading conditions. For mixed mode conditions, previous work for mode-I and mode-III fields under small-scale yielding conditions has shown complex behavior, with the in-plane stresses having a different asymptotic functional form than the out-of-plane stresses [2]. Pure mode-I, II and mixed-mode-I/II are more possible in engineering problems.

Many tests have been used to measure fracture toughness. The double cantilever beam (DCB) test [3] and compact tension specimen (CT) [4] are most often used to measure mode-I (opening) fracture toughness for composite and metallic material, respectively. The end-notched flexure (ENF) test [5] is most often used to measure mode-II (sliding shear) fracture toughness. However, crack growth in structures is usually not a result of pure mode-I or pure mode-II loading, so it is important that the fracture toughness be known for mixed-mode loading.

Several tests have been used for measuring mixed-mode fracture toughness in the mode-I/mode-II range. These tests include: the edge-delamination tension [6] the crack-lap shear [7], the mixed-mode bending (MMB) test [8], the asymmetric double cantilever beam [9], the mixed-mode flexure [10], and the variable mixed-mode [11] test. However, all of these tests have one or more problems which limit their usefulness. The modified Arcan test [12] seems to solve many of these problems. The MMB test uses a lever to simultaneously apply mode-I and mode-II type loadings, and by rotating the lever, practically any mode-I/mode-II ratio can be obtained. The Arcan test can be used with the simple and similar specimens for all in-plane mixed-mode tests and can be used to separate the mode-I and mode-II components. In other mixed-mode fracture tests, several different types of specimens are often needed to measured fracture toughness over a desired range of mixed-mode combinations. The use of different test configurations can involve different test variables and analysis procedures that can influence test results in ways that are difficult to predict. The Modified Arcan test is a test apparatus that can be used to measure fracture toughness over a wide range of mode I/II ratios as well as pure mode I and mode II.

Ductile fracture of metallic materials generally involves a stable crack growth process prior to the occurrence of unstable crack propagation. Since stable crack growth requires an increasing applied load for continued crack growth, the maximum load-carrying capacity of ductile materials may be significantly larger than the loading required initiating crack growth. Thus, conventional assessment methods using the onset of crack extension for estimating the margin of safety for flawed components manufactured from ductile materials are often overly conservative[13].

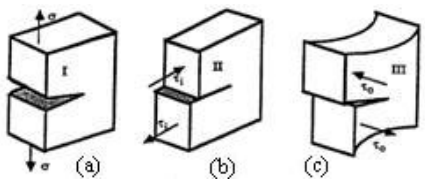

Fig. 1 (a–c) Three basic modes of fracture

Manuscript received April 30, 2008. Experimental Estimation of Fracture Properties of Steel Weld under Mixed Mode.

S. R. Hosseini is with the Civil Engineering Department, Sahand University of Technology, Tabriz, Iran (e-mail: r_hosseini@sut.ac.ir).

N. Choupani is now with the Department of Mechanics Engineering, Sahand University of Technology, Tabriz, Iran (corresponding author to provide phone: +98-412-3459051; fax: +98-412-3444300; e-mail: choupani@sut.ac.ir).

A. R. M. Gharabaghi is with the Civil Engineering Department, Sahand University of Technology, Tabriz, Iran (e-mail: mgharabaghi@sut.ac.ir).

In this study, a modified version of the Arcan specimen was redesign for the mixed-mode fracture test of high stringent specimens, which allows mode-I, mode-II, and almost any combination of mode-I and mode-II loading to be tested with the same test specimen configuration. Therefore, disadvantages presented in the previous mixed-mode toughness test methods can be avoided.

II. An Overview of Fracture Mechanics

A variety of approaches have been proposed to characterize the stable crack propagation process. For example, the J-Integral as a function of crack growth (J-R curve) has a long history of use as a crack growth resistance curve based on the studies Hutchinson and Paris (1979)[14], Paris et al. (1979)[15], and the others (e.g. Begley and Landes, 1972[16]; Clarke et al., 1976[17]). The J-integral is widely accepted as a fracture mechanics parameter for both linear and nonlinear material response. It is related to the energy release associated with crack growth and is a measure of the intensity of deformation at a notch or crack tip, especially for nonlinear materials. If the material response is linear, it can be related to the stress intensity factors. Because of the importance of the J-integral in the assessment of flaws, its accurate numerical evaluation is vital to the practical application of fracture mechanics in design calculations [18]. In ABAQUS software evaluation of J-integral is based on the virtual crack extension/domain integral methods (Parks, 1977 [19], and Shih, Moran, and Nakamura, 1986 [20]).

The purpose of fracture toughness testing is to determine the value of the critical stress intensity factor, or plane stress fracture toughness. This material property is used to characterize the resistance to fracture in the design of structural members. ASTM standards E 399 [3] and D 5045 [21] give some guidance for plane stress mode-I fracture toughness K_{IC} for metals and plastics. The stress intensity factor K_C at the tip of the pre-crack in a compact tension specimen is given by:

$$K_C = \frac{P_C}{t\sqrt{w}} f(a/w) \tag{1}$$

Where P_c is the fracture load, a is crack length, w is the specimen width, t is the specimen thickness, and $f(a/w)$ is a geometrical factor. Linear elastic fracture mechanics and plan stress conditions are the primary requirements.

The stress intensity factors ahead of the crack tip for a modified version of Arcan specimen were calculated by using the following equations [22, 23, 24 and 25]:

$$K_I = \frac{P_C\sqrt{\pi a}}{wt} f_I(a/w) \tag{2}$$

$$K_{II} = \frac{P_C\sqrt{\pi a}}{wt} f_{II}(a/w) \tag{3}$$

In turn K_{IC} and K_{IIC} are obtained using geometrical factors $f_I(a/w)$ and $f_{II}(a/w)$ respectively, which are obtained through finite element analysis of Arcan test specimen.

Also energy release rate for isotropic material with edge crack can be calculated from the following relationships:

Where E is Young's modulus and ν is Poisson's ratio.

$$G_I = \frac{K_I^2}{E} \qquad G_{II} = \frac{K_{II}^2}{E} \qquad \text{Plane stress} \tag{4}$$

$$G_I = \frac{(1-\nu^2)K_I^2}{E} \qquad G_{II} = \frac{(1-\nu^2)K_{II}^2}{E} \qquad \text{Plane strain} \tag{5}$$

III. Finite Element Background

The method used to calculate the stress intensity factor was an interaction *J*-integral method performed in ABAQUS, and is required to separate the components of the stress intensity factors for a crack under mixed-mode loading in conjunction of finite element analysis. The method is applicable to cracks in isotropic and anisotropic materials. Based on the definition of the *J*-integral, the interaction integrals J_{int}^{α} can be expressed [18]:

$$J_{\text{int}}^{\alpha} = \lim_{\Gamma\to 0}\int_{\Gamma} n.\left(\sigma : \varepsilon_{aux}^{\alpha} I - \sigma.\left(\frac{\partial u}{\partial x}\right)_{aux}^{\alpha} - \sigma_{aux}^{\alpha}.\frac{\partial u}{\partial x}\right).qd\Gamma \tag{6}$$

Where Γ is an arbitrary contour, q is a unit vector in the virtual crack extension direction, n is the outward normal to Γ, σ is the stress tensor and u is the displacement vector, as shown in Fig. 2. The subscript aux represents three auxiliary pure mode-I, mode-II, and mode-III crack-tip fields for α=I, II, III, respectively. The domain form of the interaction *J*-integral is:

$$J_{\text{int}}^{\alpha} = \int \lambda(s) n.(\sigma : \varepsilon_{aux}^{\alpha} I - \sigma.(\frac{\partial u}{\partial x})_{aux}^{\alpha} - \sigma_{aux}^{\alpha}.\frac{\partial u}{\partial x}).qdA \tag{7}$$

Where *λ(s)* virtual crack advance and *dA* is surface element. In the interaction *J*-integral method [18] the two-dimensional auxiliary fields are introduced and superposed on the actual fields. By judicious choice of the auxiliary fields, the interaction *J*-integral can be directly related to the stress intensity factors as:

$$K = 4\pi B.J_{\text{int}} \tag{8}$$

Where B is called the pre-logarithmic energy factor matrix, $J_{\text{int}} = \left[J_{\text{int}}^{I}, J_{\text{int}}^{II}, J_{\text{int}}^{III}\right]^T$ and $K = \left[K_I, K_{II}, K_{III}\right]^T$. In linear elastic fracture mechanics, the *J*-integral coincides with total energy release rate, $J = G_T = G_I + G_{II} + G_{III}$, where G_I, G_{II} and G_{III} are the energy release rates associated with the mode-I, mode-II and mode-III stress intensity factors, respectively.

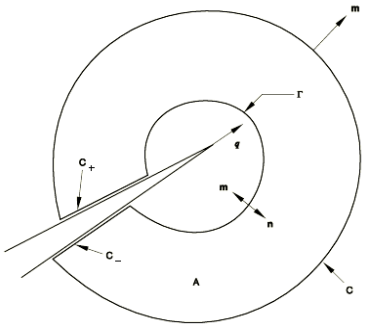

Fig. 2 Closed contour $C + C_+ + \Gamma + C_-$ encloses a domain *A* that includes the crack-tip region as $\Gamma \to 0$

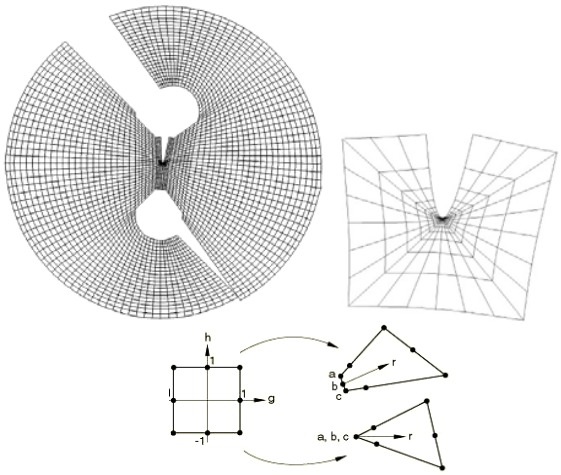

Fig. 3 Finite element mesh pattern of the entire specimen and around the crack-tip with crack length *a= 15 mm*

Numerical analyses were carried out using the interaction *J*-integral method. Fig. 3 shows example of the mesh pattern of the specimen, which were performed with ABAQUS under a constant load of 40000 N. The entire specimen was modeled using eight node collapsed quadrilateral element and the mesh was refined around crack tip, so that the smallest element size found in the crack tip elements was approximately 0.02 mm. A linear elastic finite element analysis was performed under a plain stress condition using $1/r^{0.5}$ stress field singularity. To obtain a $1/r^{0.5}$ singularity term of the crack tip stress field, the elements around the crack tip were focused on the crack tip and the mid side nodes were moved to a quarter point of each element side.

IV. Experimental Procedure

A. Specimen and Material

The material properties for S355 J2G3 high strength steel are Young's modulus, E=206 GPa, Poisson's ratio, v=0.3, σy=465 MPa and σy=549 MPa. For SFA5.1 E7018-1 electrode, E=206 GPa, v=0.3, σy= 536 MPa and σy=585 MPa. The chemical composition of this steel and weld can be seen in Table I. Specimen includes two part steel that fully welded in middle and then machined to butterfly-shape. Also, a notched has been created with wire cut as a crack which is shown in Fig. 4(b). The specimen thickness is B=8.5 mm.

TABLE I
Chemical Composition

	%C	%Mn	%Si	%S	%P	%N	%Ce
Steel	0.104	1.296	0.193	0.021	0.017	0.008	0.366
Electrode	0.07	1.460	0.290	0.004	0.009		

B. The Modified Arcan Test

The Arcan specimen and test fixture are shown in Fig. 4(a). Originally used for testing of composite specimens by Arcan et al. (1978), the fixture was modified by Amstutz et al. (1995a, 1995b) for stable tearing tests. This apparatus, also known as the modified Arcan fixture, subjects a central section of a "butterfly-shaped" specimen to homogeneous stress and strain fields, as confirmed by photoelastic analysis. Further, the stresses and deformation gradients are highest at the central section, so that failure necessarily occurs there.

The presence of a reaction force is the basic difference between the current set-up and the original Arcan fixture. In particular, increasing the number of bolts and adding hardened drill rod inserts stiffened the specimen-fixture connection. In the original design by Arcan et al. (1978), the apparatus is joined to the testing machine by a single loading pin, thus allowing rotations, resulting in zero reaction force. This may be appropriate for fiber-reinforced composites, which are relatively stiff solids. For metals, the clamped configuration was chosen for many practical reasons. Metals are in general very soft as compared to the stiff metal grips. Deformation tends to concentrate in undesirable regions of the specimen when using a single loading pin. This is due mainly to the relatively large dead weights of the half-circular metal plates. Further, a slight misalignment of the testing machine induces large out-of-plane displacements of the specimen. Therefore, a design of self-aligning intermediate grips to guide and control the planar loading process is indispensable. Authors experienced these problems when using a single loading-pin for steel materials, and showed that the problems are better solved using the clamped Arcan apparatus.

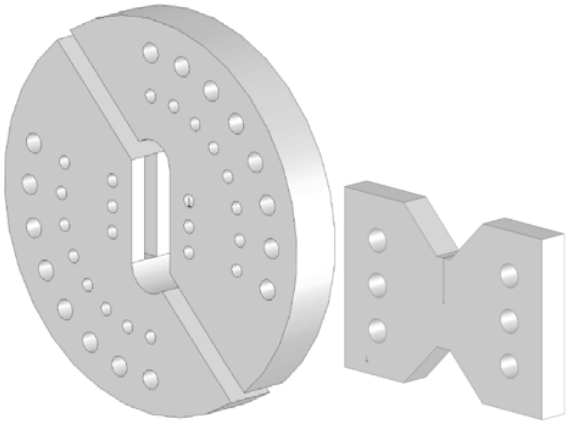

(a) (b)

Fig. 4 Specimen and Arcan apparatus

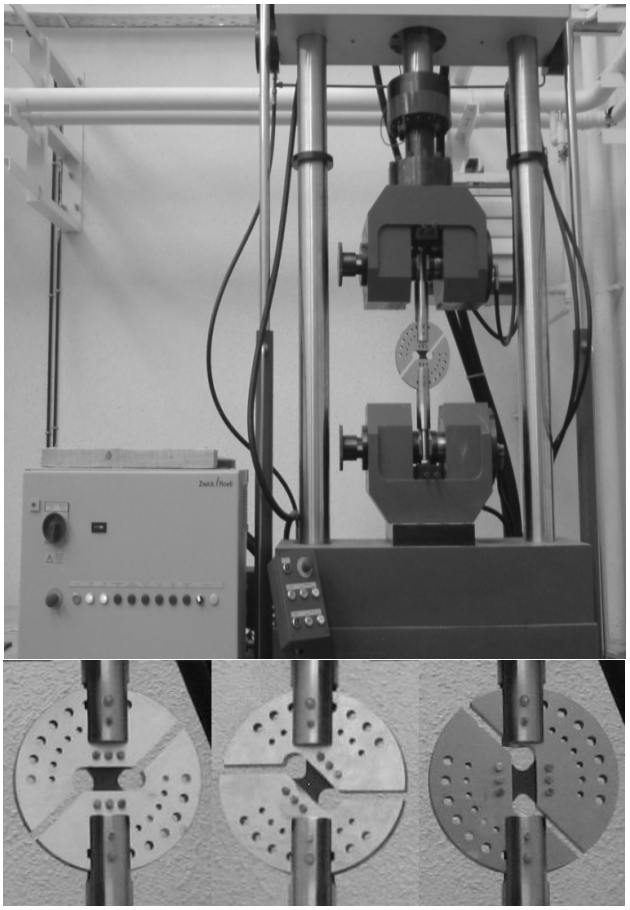

(a) (b) (c)
Fig. 5 Overview of loading device and test setup: (a) pure mode-I test; (b) mixed-mode test; (c) pure mode-II test

C. Specimen Geometry and Test Rig and Setup

Modified Arcan fixture is made of 1.6582 (DIN17200) high tensile steel with Thickness of 30mm and machined in the way to be able to test a 10mm specimen. The holes created in circumference make loading in each 15 degree possible.

The dimensions of the modified Arcan test specimen used are showed in Fig. 4 (b). Three holes were drilled along the right and left side of the specimen. Sharp crack-shaped notches were made by wire cut of 0.25mm thickness with *a/w=0.45*. For the testing of the butt welded specimens in pure mode I, pure mode II and mixed-mode loading conditions, the crack-tip extended to *a/w=0.5*. The loading device is simply installed in the universal testing machine and generates accurately repeatable loading conditions.

The specimens are colored to observe crack initiation and growth during loading process. Loading was carried out with a tensile loading device with the rate of 0.01mm per second until the final rapture.

To reduce the effects of involved errors, loading in each angle was repeated 3 times and the average was counted as final rapture load or critical load. Arcan specimen and apparatus is showed in Fig. 5.

V. Results and Discussions

A. Mixed-Mode Arcan Fracture Specimen Calibration

In order to assess geometrical factors or non-dimensional stress intensity factors $f_I(a/w)$ and $f_{II}(a/w)$ to determine fracture toughness from (2) and (3) presented in previous chapter for specimens, the *a/w* ratio was varied between 0.1 and 0.8 at 0.1 intervals and a fourth order polynomial was fitted through finite element analysis as Fig. 6:

TABLE II
Average Critical Mixed-Mode Fracture Loads P_C (N) of Butt Welded Steel for a/w=0.5

		Loading Angles		
		0°	45°	90°
Critical Loads	1	56720	53220	48310
	2	55290	52300	47580
	3	51310	45730	43940
Average		55766.7	50416.7	46610

TABLE III
Average Critical Stress Intensity Factors (K_C) ($MPa\sqrt{m}$) of Butt Welded Steel for a/w=0.5

		Loading Angles		
		0°	45°	90°
Fracture Toughness	KIC	118.1	55.13	
	KIIC		25.1	46.8

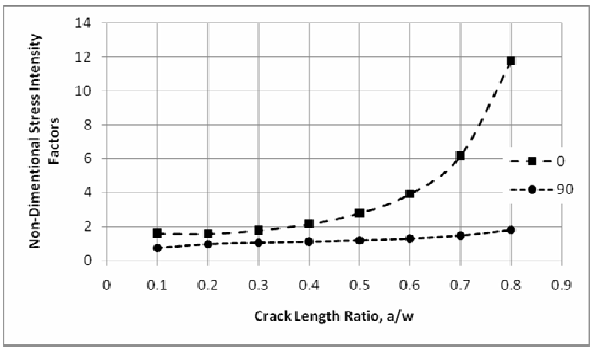

Fig. 6 Non-dimensional stress intensity factors vs. crack length of butt welded steel

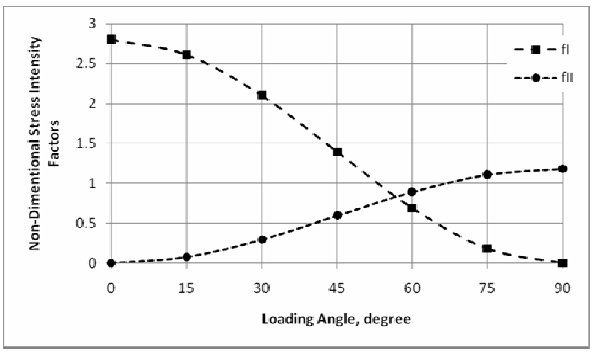

Fig. 7 Non-dimensional stress intensity factor vs. loading angle of butt welded steel for the crack length 15mm.

$f_I(a/w)(\alpha=0)=188.6(a/w)^4-260.9(a/w)^3+134.2(a/w)^2+26.3(a/w)+3.16$

$f_{II}(a/w)(\alpha=90)=-2.34(a/w)^4+12.04(a/w)^3-12.07(a/w)^2+4.977(a/w)+0.348$

Here *a/w* is the crack length ratio, where *a* is the crack length and *w* is the specimen length.

The relationship between the non-dimensional stress intensity factor and the loading angle is shown in Fig. 7. It can be seen that for loading angles $\alpha \leq 60^o$, the mode-I fracture is dominant and as the mode-II loading contribution increases, the mode-I stress intensity factor decreases and the mode-II stress intensity factor increases. For $\alpha \geq 75^o$ mode-II fracture becomes dominant.

B. Experimental Results

Fracture tests were carried out using a kind of universal tension testing machine (UTM). All tests were conducted by controlling the constant displacement rate of 0.01mm/sec in order to reduce dynamical effects and the fracture loads and displacements were recorded.

Tests were repeated 3 times for mode-I, mode-II and 45° loading angels. The load-displacement curves generated by the test machine were used to determine load vs. displacement. The tests shown some ductility and for reduce this effect specimens was colored for observe crack initiation. The average values of fracture initiation loads were used to determine the critical mixed-mode stress intensity factors. Initiation fracture toughness was determined experimentally with the modified version of the Arcan specimen under pure mode-I, II and mixed-mode loading conditions. The values of mixed-mode critical loads are shown in Table II. The average values of mixed-mode critical stress intensity factors are summarized in Table III. From Table III, It can be seen that the shearing-mode (α=90°) fracture toughness is smaller than the opening-mode (α=0°) fracture toughness. This means that the cracked specimen is tougher in tensile loading conditions and weaker in shear loading conditions.

Also Fracture toughness measurements for the modified Arcan specimen under pure mode-I loading show the average fracture toughness of $K_{IC}=(K_I)_C=118.1$ [MPa.m$^{1/2}$] for steel butt welded with crack length 15mm. For pure mode-II loading using modified Arcan specimen, the average fracture toughness is found $K_{IIC}=(K_{II})_C=46.8$ [MPa.m$^{1/2}$].

VI. Conclusion

In this paper the mixed-mode fracture behavior of steel butt weld specimens was investigated based on experimental and numerical analyses. A modified version of Arcan specimen was employed to conduct a mixed mode test using the special test loading device. It is a simple test procedure, clamping/unclamping the specimens is easy to achieve and only one type of specimen is required to generate all loading conditions. Finite element analysis confirmed that by varying the loading angle of Arcan specimen pure mode-I, pure mode-II and a wide range of mixed-mode loading condition can be created and tested. The fracture toughness was determined experimentally with the modified version of the Arcan specimen under mixed-mode loading condition. Results indicated that the cracked specimen is tougher in opening loading condition and weaker in shear loading condition.

Acknowledgment

The authors wish to thank Mr. Banaei the head of SADRA, Inc. who provided us with this kind of steel and preparing and quality control of the specimens.

References

[1] Lawn BR, Wilshaw TR. Fracture of brittle solids. London: Cambridge University Press, 1975.
[2] Michael A. Sutton, Michael L. Boone, Fashang Ma, Jeffrey D. Helm, A combined modeling-experimental study of the crack opening displacement fracture criterion for characterization of stable crack growth under mixed mode I/II loading in thin sheet materials; Engineering Fracture Mechanics 66 (2000) 171-185
[3] Wilkins, D. J.; Eisenmann, J. R.; Camin, R. A.; Margolis, W. S.; Benson, R. A.; Characterizing Delamination Growth in Graphite-Epoxy, Damage in Composite Materials, ASTM STP 775, K. L. Reifsnider, Ed., American Society for Testing and Materials, Philadelphia, 1982, pp. 168-183.
[4] American Society for Testing and Materials. 2007. Standard E399-06, Standard Test Method for Linear-Elastic Plane-Strain Fracture Toughness KIC of Metallic Materials. Annual Book of ASTM Standards. Philadelphia: ASTM.
[5] Russell, A. J.; On the Measurement of Mode II Interlaminar Fracture Energies, DREP Materials Report. 82-0, Defense Research Establishment Pacific, Victoria, December, 1982.
[6] O'Brien, T. K.; Mixed-Mode Strain-Energy-Release Rate Effects on Edge Delamination of Composites, Effects of Defects in Composite Materials, ASTM STP 836, D. J. Wilkins, Ed., American Society for Testing and Materials, Philadelphia, 1984, pp. 125-142.
[7] Johnson, W. S.; Stress Analysis of the Crack-lap-Shear Specimen: An ASTM Round-Robin, Journal of Testing and Evaluation, JTEVA, Vol. 15, No.6, November 1987, pp. 303-324.
[8] Reeder, J. R.; and Crews, J. H., Jr.; The Mixed-Mode Bending Method for Delamination Testing, AIAA Journal, Vol. 28, No.7, July 1990, pp. 1270-1276.
[9] Bradley, W. L.; and Cohen, R. N.; Matrix Deformation and Fracture in Graphite-Reinforced Epoxies, Delamination and Debonding of Materials, ASTM STP 876, W. S. Johnson, Ed., American Society for Testing and Materials, Philadelphia, 1985, pp. 389-410.
[10] Russell, A J.; and Street, K. N.; Moisture and Temperature Effects on the Mixed-Mode Delamination Fracture of Unidirectional Graphite/Epoxy, Delamination and Debonding of Materials, ASTM STP 876, W. S. Johnson, Ed., American Society for Testing and Materials, Philadelphia, 1985, pp. 349-370.
[11] Hashemi, S.; Kinloch, A. J.; and Williams J. G.; Interlaminar Fracture of Composite Materials, 6th ICCM & 2nd ECCM Conference Proceedings, Vol. 3, London, July 1987, pp. 3.254-3.264.
[12] Arcan, M.; Hashin, Z.; and Voloshin, A., A Method to Produce Uniform Plane- Stress States with Applications to Fiber-Reinforced Materials, Experimental Mechanics, Vol. 28, April 1978, pp. 141-146.
[13] M. A. Sutton and et al. Development and application of a crack tip opening displacement-based mixed mode fracture criterion, International Journal of Solids and Structures 37 (2000) 3591-3618.
[14] Maccagno, T.M. and Knott, J.P. The low temperature brittle fracture behaviour of steel in mixed modes I and II, Engineering Fracture Mechanics, 1991, 38, 111-128.
[15] Shih, C.P. Small-scale yielding analysis of mixed-mode plane-strain crack problems, In Fracture Analysis, ASTM STP 560, American Society for Testing and Materials, Philadelphia, 1974, PA, 187-210.
[16] Hutchinson, I.W., Paris, P.C., Stability analysis of I-controlled crack growth, Elastic-plastic fracture ASTM STP, 1979, 668, 37-64.
[17] Paris, P.C, Taha, H., Zahoor, A., Ernst .19, H., The theory of instability of the tearing mode of elastic-plastic crack growth, Elastic-plastic fracture ASTM STP, 1979, 668, 5-36.
[18] ABAQUS user's manual, version 6.5. Pawtucket, USA: Hibbit, Karlsson and Sorensen, HKS Inc; 2004.
[19] Nagtegaal, J. C., D. M. Parks, and J. R. Rice, On Numerically Accurate Finite Element Solutions in the Fully Plastic Range, Computer Methods in Applied Mechanics and Engineering, vol. 4, pp. 153–177, 1977.

[20] Shih, C. F., B. Moran, and T. Nakamura, "Energy Release Rate along a Three-Dimensional Crack Front in a Thermally Stressed Body," International Journal of Fracture, vol. 30, pp. 79–102, 1986.
[21] ASTM D5045, Standard Test Method for Plane Strain Fracture Toughness and Strain Energy Release Rate of Plastic Materials: Annual Book of ASTM Standards, 1995.
[22] Choupani, N. "Experimental and Numerical Investigation of the Mixed-Mode Delamination in Arcan Laminated Specimens", International Journal of Materials Science & Engineering A. volume 478(2008): 229-242.
[23] P.M. Noury, R.A. Shenoi and I. Sinclair, "On mixed-mode fracture of PVC foam", International Journal of Fracture vol. 92, p. 131–151, 1998.
[24] R. A. Jurf, R. B. Pipes, "Intergranular Fracture of Composite Materials", J. Composite Materials, vol. 16, p. 386-394, 1982.
[25] E. E. Gdoutos, D. A. Zacharopoulos, and E. I. Meletis, "Mixed-Mode Crack Growth in Anisotropic Media", Engineering Fracture Mechanics, vol. 34(2), p. 337-346, 1989.